

# Efficient Wood Hydrophobization Exploiting Natural Roughness Using Minimum Amounts of Surfactant-Free Plant Oil Emulsions

Jan Janesch, Claudia Gusenbauer, Andreas Mautner, Wolfgang Gindl-Altmutter,\* and Christian Hansmann



Cite This: *ACS Omega* 2021, 6, 22202–22212



Read Online

ACCESS |



Metrics & More

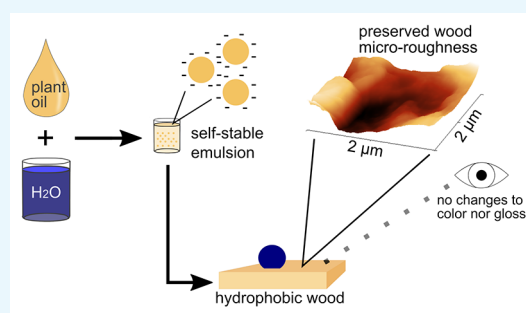


Article Recommendations



Supporting Information

**ABSTRACT:** Wood in service requires protection from excessive moisture. Herein, we demonstrate that efficient surface hydrophobization can be provided with small amounts of biobased oils, benefitting from the hierarchical roughness inherent to wood surfaces. The developed technique involves coating spruce wood with surfactant-free emulsions based on tung oil, linseed oil, or a linseed oil-based long oil alkyd resin. The  $\zeta$ -potential of the emulsions was determined by electrophoretic mobility measurements. X-ray photoelectron spectroscopy (XPS), scanning electron microscopy (SEM), atomic force microscopy (AFM), and spectrophotometry were used to study coated surfaces. XPS measurements confirmed the presence of the tung oil coatings. Tung oil emulsions were effective at concentration levels as low as 0.04 wt % oil content, roughly equivalent to  $0.04 \text{ g m}^{-2}$  and led to static water contact angles reaching up to  $>130^\circ$ . SEM imaging and AFM measurements provide evidence that the micro- and nanostructures inherent to wood enhance the hydrophobization effect of the obtained coatings. A further benefit of the method lies in only minimal effects of the coating on the surface color and gloss. Thus, the mass-efficient process following several of the principles of green engineering led to improved water repellency while not affecting the visual appearance of the coated wood.



## INTRODUCTION

Being a mechanically strong, versatile, renewable, and esthetic material, wood remains a highly popular choice for diverse applications. Unfortunately, susceptibility to uptake water due to its essentially hydrophilic biopolymer character diminishes its dimensional stability and decay resistance.<sup>1,2</sup> Surface treatments offer a cost-effective way to prevent or delay water uptake. Several classes of coating materials have been developed for this purpose, involving binders of a big variety of different chemistries. These include but are not limited to acrylic, polyurethane, epoxy, and vinyl resins,<sup>3</sup> all of which are of petrochemical origin. To preserve the renewable character of wood, which is one of the strongest arguments for its use, coating materials matching the renewable and the minimal environmental impact character of wood should be given priority. Drying oils and natural resins such as waxes are the two major biobased substance classes used for wood hydrophobization.<sup>3</sup> Waxes suffer from thermal instability due to their low melting temperature, leaching, and low abrasion resistance.<sup>3,4</sup> Moreover, the preparation of wax emulsions usually involves heating of the wax prior to dispersion.<sup>4–8</sup> Drying oils such as tung oil, linseed oil, as well as biobased synthetic alkyds hold several advantages over waxes. Their high content of triglyceride esters of unsaturated fatty acids endows them with the ability to cross-link after deposition on and penetration of the wood surface. Moreover, drying oil coatings

partially preserve the natural moisture buffering ability of wood, a desired property in construction, which is usually decreased when using lacquer or a wax film.<sup>6</sup> Figure 1 shows the structures of  $\alpha$ -linolenic acid (Figure 1a) and  $\alpha$ -eleostearic acid (Figure 1b), the two most represented fatty acids contained in linseed oil and tung oil, respectively.

Alkyds are polyester resins derived from the polymerization of fatty acids, a polyol such as glycerol, and a dibasic acid in a condensation reaction. One way to obtain alkyds is the monoglyceride process described in Figure 1c. The process involves transesterification of triglycerides with glycerol to obtain monoglycerides. These are then reacted in a second step with a polybasic acid, such as phthalic anhydride, to obtain alkyds. Oxidizing alkyds are known for their improved cross-linking properties. Though known since the 1920s, this type of binder has recently regained popularity, not least because of the high biobased content as well as its biodegradability.<sup>9</sup> Long oil alkyds contain more than 60% of oils, such as linseed oil or soybean oil, and can therefore easily reach a biobased content

Received: June 2, 2021

Accepted: July 29, 2021

Published: August 17, 2021



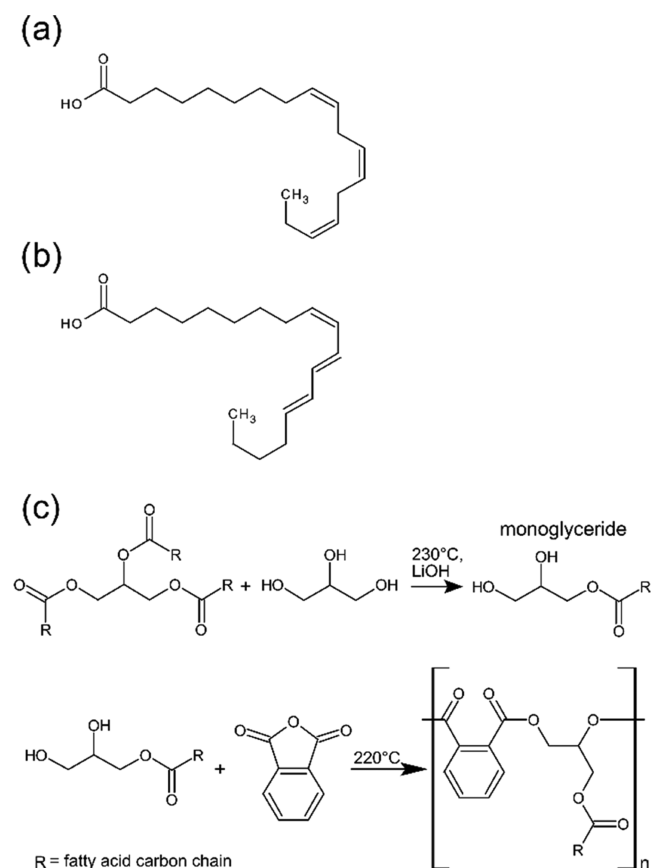


**Figure 1.** Chemical structures of  $\alpha$ -linolenic acid (a) and  $\alpha$ -eleostearic acid (b). Synthesis of alkyd resin by the reaction of triglycerides, glycerol, and phthalic anhydride in the monoglyceride process (c).

of more than 70%, if glycerol or other biobased polyalcohols are used. Recent efforts aim at replacing the fossil-based dibasic acid by greener alternatives to further increase the content of renewable carbon in alkyd resins.<sup>10</sup>

Despite the advantages of drying oils and alkyds over waxes, their limited inherent hydrophobicity, with water contact angles (WCAs) on wood even in the hydrophilic region of  $<90^\circ$  being reported for drying oils,<sup>6,11</sup> limit their use as effective water repellents. Nonetheless, moderate protection of the wood surface is achieved. A significant enhancement of the effective water repellency of a smooth hydrophobic surface can be acquired by an increase in its surface roughness. Techniques to achieve this include the deposition of nanoparticles by different means or direct growth of nanostructures on the substrate<sup>12–15</sup> as well as phase separation and templating processes.<sup>16,17</sup> Inspired by this, we have recently used tung oil as a partial substitute for beeswax in the preparation of wood surfaces with WCAs  $>150^\circ$  and WCAs as high as  $136^\circ$  when using a pure tung oil coating.<sup>18</sup> This was achieved using a templating method to provide a specific level of surface roughness in the micrometer range. Unfortunately, many techniques providing rough water-repellent surfaces involve the deposition of nanoparticles, which may pose risks to human beings and the environment due to unresolved toxicological questions.<sup>19</sup> Moreover, a decrease in the esthetic properties is an often-encountered side effect when increasing the surface roughness, leading to loss of transparency and whitening of the surface due to scattering effects.<sup>8,20–22</sup> This trade-off between wettability and transparency is a well-known challenge in materials science.<sup>23</sup> Because wood is especially valued for its esthetic appeal, changes to its appearance are undesired.

The fact that wood is not flat and smooth, but per-se a hierarchical structure with inherent roughness at several levels of scale is well known but rarely in the spotlight. We propose that this roughness may be beneficially exploited toward enhancing the hydrophobization effect of drying oil under the condition that only small amounts, which do not diminish roughness, are applied. Such an approach was demonstrated feasible by grafting of long-chain alkyl groups to wood's hydroxyl groups using a solution of stearyl chloride in toluene, leading to water contact angles of  $138^\circ$  and  $152^\circ$  on the radial and transverse surfaces, respectively.<sup>24</sup> Similarly, dilute poly(dimethylsiloxane) (PDMS) -emulsions were used to

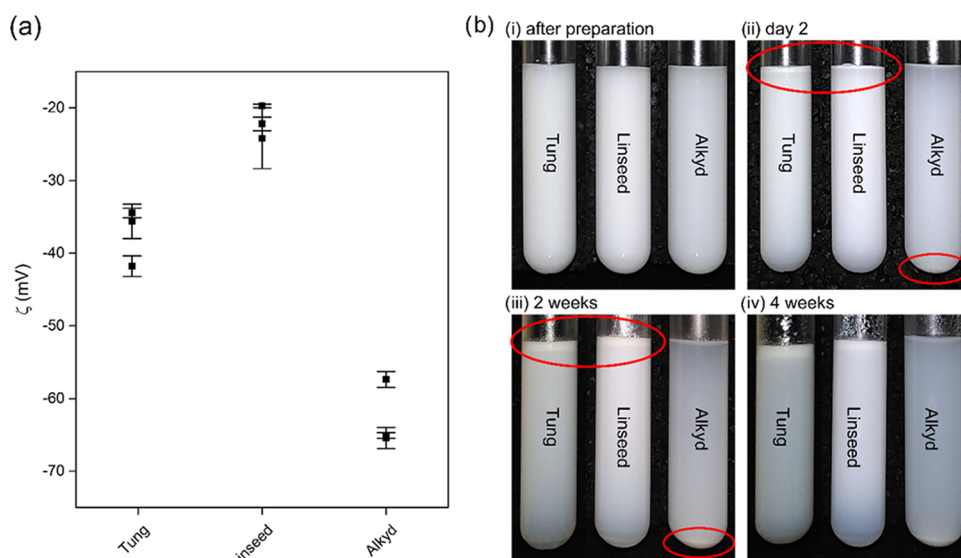


**Figure 2.** (a)  $\zeta$ -Potential values measured for the three oil emulsions. Points and error bars are the arithmetic mean and standard deviation of triplicate measurements. (b) Pictures of emulsions of 1 g of oil in 99 g of water taken at different time intervals. Red ellipses highlight creamed tung oil and linseed oil and sedimented alkyd resin.

obtain superhydrophobic cotton fabrics by increasing their inherent roughness.<sup>25</sup> Changing to water in form of an emulsion-based process could render such an approach highly mass-efficient. This is also encouraged in the light of environmental legislations regarding volatile organic compound (VOC) regulations.<sup>26</sup> While conventional emulsion technology requires the use of surface-active agents, recent studies have reported self-stable wax dispersions for use in wood coatings, thereby omitting potentially harmful surfactants.<sup>7,8</sup> In addition, the feasibility of self-stable plant oil emulsions has been demonstrated.<sup>27,28</sup>

In the present study, we investigate the preparation of self-stable surfactant-free emulsions based on drying oils and alkyds and evaluate their applicability for wood hydrophobization. Particular emphasis is placed on the role of inherent roughness with regard to the degree of hydrophobization provided.

## RESULTS AND DISCUSSION

**Emulsion Characterization and Stability.** Figure 2a shows plots of the results of  $\zeta$ -potential measurements. Low scattering within groups demonstrates good repeatability. Values were negative throughout and varied between  $-20$  and  $-30$  mV for linseed oil and  $-35$  to  $-45$  mV for tung oil, while alkyd resins showed lower  $\zeta$ -potential values at around  $-65$  mV. The measured negative  $\zeta$ -potential is in general agreement with the literature on surfactant-free plant oil emulsions. For surfactant-free emulsions of glycerol trioleate and sunflower oil,  $\zeta$ -potential values of  $-30$  mV and between  $-60$  and  $-73$  mV, respectively, have been reported.<sup>27,28</sup> Accumulation of  $\text{OH}^-$  ions at the water/oil interface is believed to be a general stabilization mechanism for surfactant-free o/w emulsions of oils with low solubility in water.<sup>29</sup> For plant oil emulsions, a pH drop correlating with sonication time has been detected, indicating that  $\text{OH}^-$  ions adsorbed at the surface.<sup>28</sup> This is in agreement with Beattie and Djerdjev, who found that the amount of NaOH necessary to maintain the pH of o/w emulsions correlated with the droplets surface area.<sup>29</sup> This mechanism might also explain the negative  $\zeta$ -potential of the emulsions prepared in the present study. In addition to this, the negative charge could also result from free fatty acid contained in the oils. The carboxylic acid groups of oleic acid, linoleic acid, and  $\alpha$ -linolenic acid have  $\text{pK}_a$  values of 8–10.<sup>30</sup> Their partial dissociation could contribute to the  $\zeta$ -potential.<sup>27</sup> In the alkyd, the negative charge could also be due to unreacted carboxylic acid groups and hydroxyl groups. This could help to explain why the alkyd resin reached lower  $\zeta$ -potential values compared to the linseed oil, which it is derived from.

Trials for testing of the droplet size of emulsions by dynamic light scattering revealed a high polydispersity index (PDI) as well as sedimentation or agglomeration processes, making an accurate determination impossible. Because of the suspected impact on emulsion stability, emulsions were prepared without siccatives and their stability was visually determined (Figure 2b). On the second day after preparation, partial visible separation was apparent in all emulsions, as indicated by red circles in Figure 2bii. The densities of 0.93, 0.94, and 1.04 g/mL for linseed oil, tung oil, and the alkyd resin, respectively, reflect the separation behavior by gravity. Being lighter than water, tung oil, and linseed oil emulsions showed creaming to the top. On the other hand, the alkyd—being heavier than water—showed sedimentation to the bottom. This separation became more pronounced with time (Figure 2biii). However,

4 weeks after preparation, all resins were still partially dispersed (Figure 2biv). This demonstrates the general possibility to prepare storable self-stable emulsions. Stokes' law states that creaming and sedimentation velocity increase with the second power of the droplet size.<sup>31</sup> Thus, larger droplets inside the emulsion are the likely cause for the apparent separation under earth gravity. Testing the droplet size of one tung oil emulsion sample after 1 week of storage gave good measurement quality and a z-average diameter of 300–330 nm. It thus seems that at low droplet sizes, electrostatic repulsion stabilizes the emulsion over extended periods. To obtain storable emulsions, we propose to decrease the particle size further, e.g., by longer sonication times.

**Surface Elemental Composition by X-ray Photoelectron Spectroscopy (XPS) Measurements.** X-ray photoelectron spectroscopy was carried out to investigate the surface chemistry of uncoated spruce wood, spruce wood coated with Emulsion-C and spruce wood coated with pure tung oil. Regarding the elemental composition, it was found that the surface of all three variants did mainly consist of carbon and oxygen, as expected. Uncoated wood (Figure 3) possessed a C/O ratio of 65:35 atom % and minute amounts of nitrogen, owing to its composition consisting mainly of cellulose, hemicellulose, and lignin, typical for wood surfaces.<sup>32,33</sup> This C/O ratio increased to 71:29 for Emulsion-C coating and 79:20 for pure tung oil coatings, respectively. This indicates the presence of compounds, which contain a higher ratio of carbon to oxygen compared to the typical wood constituents. Because tung oil mainly consists of carbon-rich fatty acids,<sup>18</sup> this result supports the conclusion that coating with a tung oil emulsion and pure tung oil led to successful disposition of oil on the wood surface. Peaks indicating Zr and Al were also detected in both coatings. Additionally, Fe was detected in pure tung oil coatings. These three elements were contained in the drying agents added to the oil to catalyze autoxidative cross-linking. Their presence further evidences the presence of a coating.

A deconvolution of the C 1s peak for all three types of samples is presented in Figure 3. Peaks at 284.8,  $\sim 286.5$ ,  $\sim 288$ , and  $\sim 289$  eV correspond to C–C/C–H, C–O, O–C–O/C=O, and O–C=O, respectively. The results reflect the trend observed for the elemental composition: uncoated wood (Figure 3a) had a ratio of C–C to C–O of 37:47, typical for wood. This was turned in favor of C–C bonds for wood coated with Emulsion-C (Figure 3b), as indicated by a ratio of 53:35. An even stronger dominance of the C–C bonds over C–O bonds with a ratio of 75:14 was evident for the pure tung oil coating (Figure 3c). Tung oil contains a tail of aliphatic C–C bonds, which increases the fraction of C–C present over C–O bonds. The results of elemental composition and the deconvolution of the C 1s peak also suggest that the pure tung oil coating resulted in the deposition of more oil onto the wood surface compared to the emulsion-based coating.

**Results of Water Contact Angle Measurements.**  
*Hydrophobic Performance of Tung Oil Emulsion Coatings.* The coating of wood with tung oil at various concentrations resulted in clear effects on wettability with water. Figure 4a shows static water contact angles (WCA). Specimens coated with pure tung oil and uncoated spruce specimens are found at a concentration of 100 and 0 wt %, respectively, whereas emulsion-coated specimens cover the space between these two extremes.

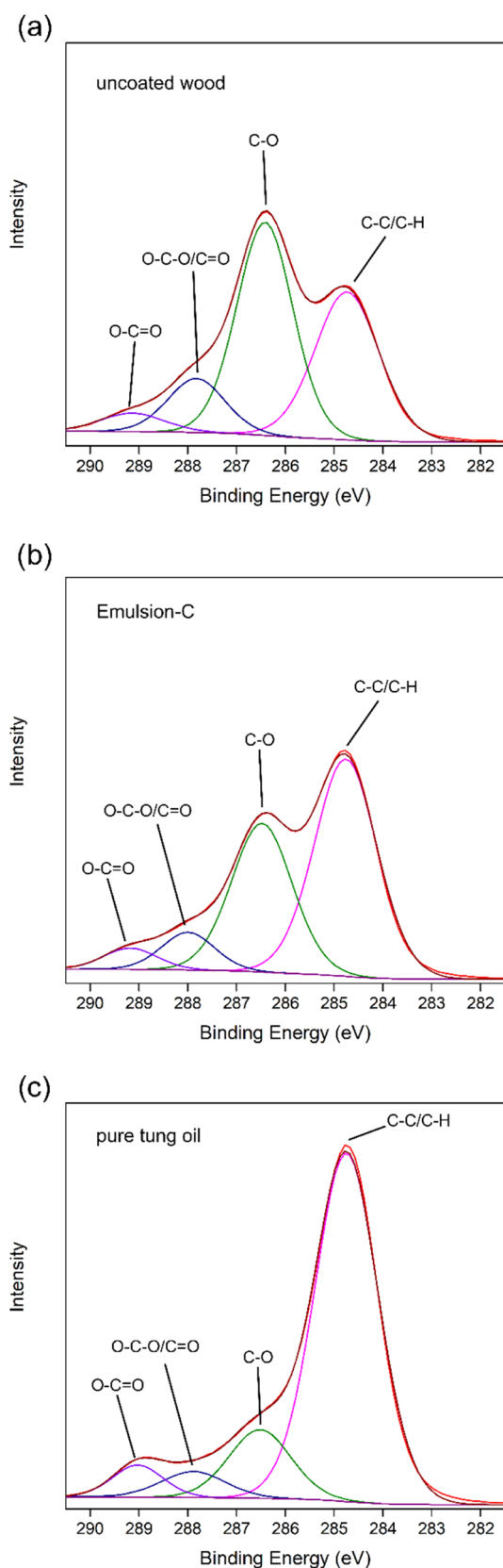


**Figure 3.** Deconvolution of the C 1s spectra obtained by X-ray photoelectron spectroscopy of uncoated spruce wood (a) and spruce wood coated with tung oil Emulsion-C (b) or pure tung oil (c).

Samples coated with pure tung oil (100 wt %) showed WCAs around 90°, which is in a similar range as the

hydrophobic properties reported by Arminger et al. who found WCA between 90 and 100° on beech and oak wood.<sup>11</sup> Using comparably high oil content, Emulsions-D and -E led to improved water repellency compared to pure tung oil coatings. An optimum hydrophobization effect was observed for the more dilute Emulsion-C (~0.16 wt % oil content) and Emulsion-D (~0.04 wt % oil content). On spruce coated with the most dilute Emulsion-A (~0.01% oil content), water contact angles rapidly declined during measurement and water penetrated the samples' surface. Nevertheless, such coatings still imparted surfaces with slightly improved hydrophobic properties compared to native wood samples.

Notably, significant surface protection was achieved with surface coverage as low as 0.04–0.15 g m<sup>-2</sup>. Considering that application rates of industrially applied systems can be more than 120 g m<sup>-2</sup><sup>34</sup> and taking into account the far higher oil contents of commercial wood coatings,<sup>35</sup> this corresponds to a reduction of solids applied by a factor of 10–1000.

**Time-Stability of Water Contact Angles on Coated Spruce Wood.** Consistency of the water repellency was assessed by measuring the contact angle of one water droplet for 120 s at intervals of 2 s. Figure 4b depicts one exemplary curve for every tung oil emulsion type as well as pure tung oil coatings. The contact angle reduction factor  $F_{CAR,m}$  originally established to monitor the cross-linking progress of drying oils on wood surfaces, is a way to quantify the decrease of the water contact angle over time.<sup>8</sup>  $F_{CAR,100}$  was calculated here as the difference of the  $WCA_0$  at  $t = 0$  s and the  $WCA_{100}$  at  $t = 100$  s divided by the initial water contact angle  $WCA_0$ .  $F_{CAR,100}$  of spruce coated with the dilute Emulsion-A (~0.01% oil content) showed a decline of  $WCA_0$  of up to 40% during the first 100 s of measurement. The stability over the course of 120 s of the water repellency of all other emulsion coatings, which had a higher oil content, was in a comparable range to pure oil coatings, showing  $F_{CAR,100} < 5\%$ .

When monitoring water droplets on wood coated with Emulsion-D, Emulsion-C, and pure tung oil over the course of 30 min, a considerable decrease of the WCA was detected for all three tested specimens (Figure S1). The coating based on Emulsion-C had fully absorbed the droplets before the end of the testing time. Droplets on a coating based on Emulsion-D experienced a decrease of the initial WCA by around 45–50% and a reduction in droplet volume of ~80%. For a pure tung oil coating, the initial WCA decreased by ~45% and the droplet volume decreased by 64–65%. Considering the small sample size, a more detailed investigation would be necessary to draw solid conclusions. However, these results suggest, that while coating wood with diluted oil emulsions can achieve high initial WCAs, pure tung oil coatings might still offer a better protective barrier against the penetration of water into the wood, when looking at extended periods of time.

**Effect of Surface Preparation.** Machining processes such as sanding and planing change the surface structure and consequently the roughness of wood. Moreover, it has been shown that sanding has an impact on the contact angle of uncoated wood.<sup>36</sup> To study the effect of wood machining on the hydrophobic properties of coated wood, this experiment compared the static WCA of sanded and planed wood samples after bath coating with tung oil emulsions (Figure 5a). Gravimetric analysis revealed oil contents of 0.74 and 0.16 wt % for Emulsion-D and Emulsion-C, respectively. In both groups (sanded and planed), Emulsion-C showed superior water repellency compared to Emulsion-D, which confirms the

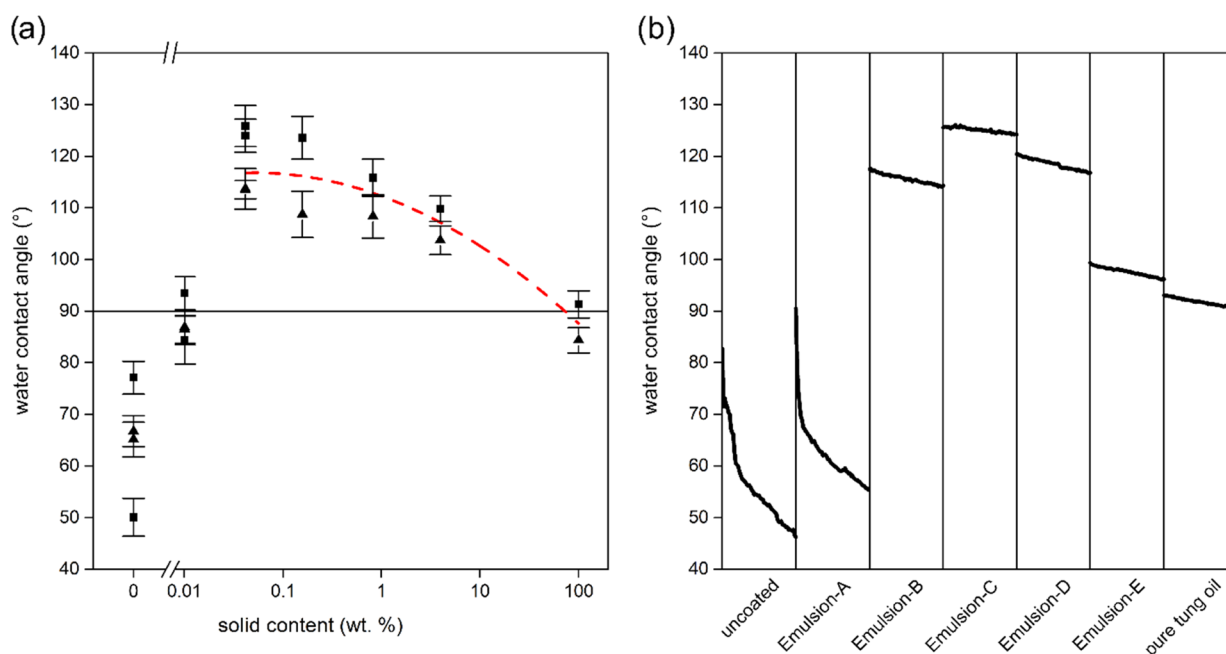


**Figure 4.** Specimen wettability with water determined by static contact angle measurement. (a) Static water contact angle of coated and uncoated spruce surfaces as a function of oil content. The  $x$ -axis represents different oil contents of coatings as determined by gravimetric analysis. The arithmetic mean and 95% confidence interval of measurements of seven random locations per specimen is shown for samples cut from two different logs, distinguished by squares and triangles. The red curve shows a second-order polynomial fit calculated from all samples except Emulsion-A and uncoated samples. (b) Exemplary curves showing the stability of the contact angle of a droplet monitored for 120 s.

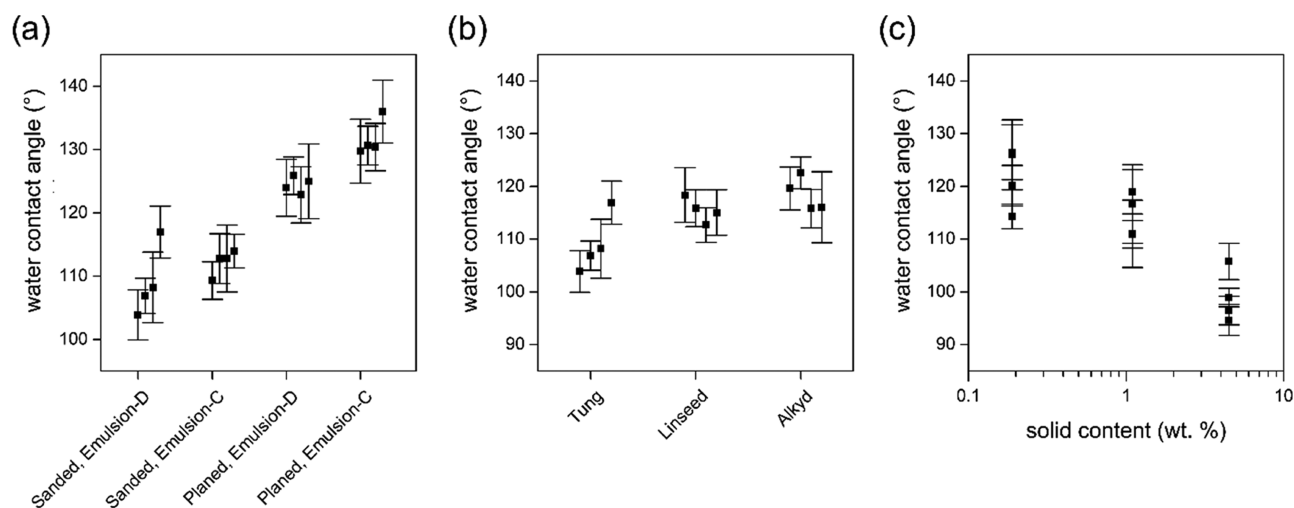


**Figure 5.** (a) Static WCA of planed vs sanded wood coated with Emulsion-D (from 1 g of an oil mixture in 99 g of water) and Emulsion-C, obtained by 5-fold dilution of Emulsion-D. (b) Static WCA on spruce wood coated with Emulsion-D of tung oil, linseed oil, and alkyd resin. (c) Static WCA of droplets of  $\sim 8 \mu\text{L}$  as a function of the oil content after spray coating of spruce wood. Points represent the mean of seven measurements on individual spruce specimens. Error bars show the 95% confidence interval.

previous observation that up to a certain extent, lower oil content provides more efficient hydrophobization (Figure 4). Moreover, planed surfaces outperformed sanded surfaces with mean contact angles of about  $130^\circ$  and individual contact angles exceeding  $140^\circ$ . We attribute this improved hydrophobic performance to the increased surface area as a result of higher microscale roughness (see the [Scanning Electron Microscopy Imaging](#) section). Strictly speaking, the Young–Laplace equation is limited to smooth surfaces. Here, it was nevertheless applied to measure WCAs on rough planed surfaces because it should still give the best fit and enables comparison to sanded wood surfaces.

**Comparing Different Oils.** To assess whether the developed process was similarly efficient with other emulsions than tung oil, bath coating of spruce specimens was also performed with emulsions prepared from linseed oil and the alkyd resin. Emulsions were prepared by the procedure described above, diluting 1 g of the mixture of resin and siccatives with 99 g of deionized water. The gravimetric analysis found 0.70, 1.02, and 0.74 wt % oil content for emulsions prepared from tung oil, linseed oil, and alkyd resin, respectively. Preparation and application of all three emulsions were similar. This was also true for hydrophobic properties of coated samples (Figure 5b).

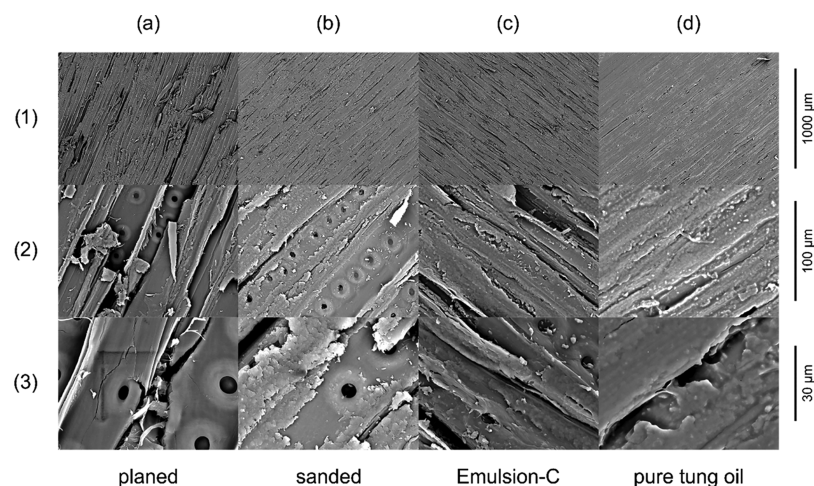


**Figure 6.** Scanning electron microscopy images of uncoated planed wood (a), uncoated sanded wood (b), and wood coated with low solid-content Emulsion-C (c) or pure tung oil (d) at three different magnifications (1–3).

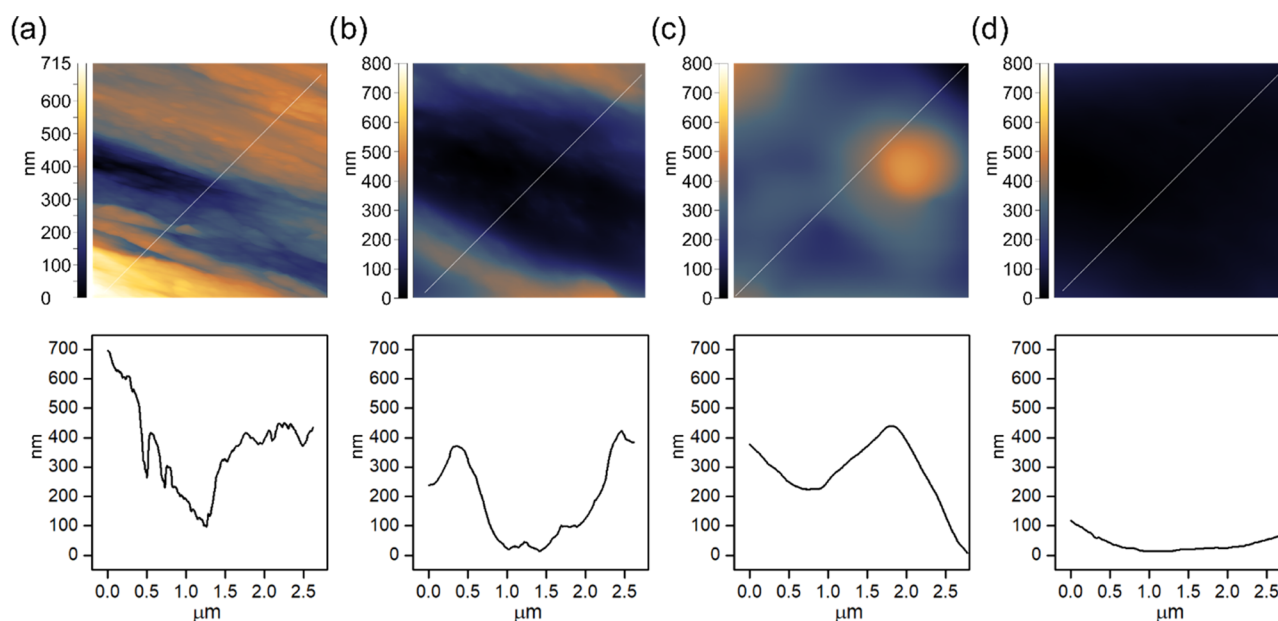


**Figure 7.** Exemplary AFM images (top) and surfaces profiles (bottom) along a diagonal line for native spruce wood (a) and spruce coated with Emulsion-C (b), Emulsion-E (c), and pure tung oil (d).

All emulsions equipped spruce wood with comparable water repellency, indicated by WCAs between 100 and 125°.

**Effect of the Application Procedure.** An industrial spraying process was simulated on a laboratory scale by applying tung oil emulsions of different concentrations with a spray gun onto spruce wood moving at a defined speed. Spraying was successful using Emulsion-E, Emulsion-D, and Emulsion-C (4.5, 1.1, and 0.2 wt %, respectively). As Figure 5c shows, this led to the same hydrophobization trend observed for bath coating (Figure 4a), with more dilute emulsion concentrations outperforming more concentrated emulsions.

Moreover, it was possible to brush coat tung oil emulsions Emulsion-D and Emulsion-C onto spruce wood, oak wood, and beech wood and achieve comparable water-repellent properties. This suggests the applicability to other types of wood and a potential for the DIY sector, where brushing is one of the most important application techniques.

**Surface Topography by Scanning Electron Microscopy (SEM).** Figure 6 shows electron microscopy images of uncoated

wood samples and wood samples coated with tung oil emulsions or pure tung oil. This was carried out to gain an impression of the surface topography and possible changes to it as a result of coating. Images of planed wood surfaces (Figure 6a) show open-lumen channels with cell-wall ridges at a distance of 20–50 μm, causing a characteristic microgrooved topography. Partial flattening by sanding (Figure 6b1) led to a smoother surface compared to planed surfaces (Figure 6a1). Increasing magnification, revealed fine-scale structures in sanded wood (Figure 6b2,b3). Microstructures on this magnification level were still well visible after coating the surface with Emulsion-C, a tung oil emulsion with a ~0.16 wt % oil content (Figure 6c2,c3). In contrast, coating the surface with pure tung oil seemed to change the topography by covering and obscuring small-scale surface structures (Figure 6d2,d3).

Because higher surface roughness increases the water repellency of a hydrophobic coating, the observations made in SEM are in good agreement with the results of contact angle

measurements (Figure 4a). The open-lumen structure could explain the higher WCA measured on planed surfaces compared to sanded surfaces (Figure 5a). Following this argumentation, coating wood with pure tung oil probably covered small-scale surface structures, thereby decreasing the surface area. This could serve as an explanation for the smaller initial WCA of pure tung oil coatings compared to emulsion coatings.

**Surface Topography and Roughness by Atomic Force Microscopy (AFM).** Atomic force microscopy was used to scan native and coated spruce wood to gain insight into the topography on a nano- and submicron level. Accordingly, a scan size of  $2 \times 2 \mu\text{m}^2$  was chosen. Figure 7 shows AFM height maps and surface profiles along a diagonal line of native spruce wood (Figure 7a) and spruce wood coated with tung oil emulsions Emulsion-C (Figure 7b), Emulsion-E (Figure 7c), and pure tung oil (Figure 7d). The characteristic fibrous wood structure originating from the orientation of cellulose fibrils appears on the surface of uncoated spruce wood (Figure 7a). They approximately match the dimensions of aggregates of microfibrils, which were determined to be between 15 and 20 nm.<sup>37</sup> This structuration on the nanometer scale was less pronounced but still detectable in wood coated with tung oil emulsions Emulsion-C (Figure 7b) and Emulsion-E (Figure 7c), respectively. However, such rough topography was generally absent in pure tung oil coatings (Figure 7d). This supports the hypothesis from observations in SEM that higher oil content masked the inherent nano- and submicron structure of the native wood surface. Figure 7 presents only a selection of images. All AFM images measured in this study can be found in the Supporting Information and give the reader a more diverse impression.

AFM was also used to determine the roughness factor  $R_f$ , which is defined as the ratio of the actual surface area  $A$  to the flat projected area  $A_0$  eq 1.

$$R_f = \frac{A}{A_0} \quad (1)$$

AFM is a widely applied tool to obtain the surface area of rough objects.<sup>38–40</sup> Here, the surface area was determined by applying a triangulation algorithm to the AFM height data. The calculated roughness factors of native and coated spruce wood are plotted in Figure 8. The high scattering is explained by the anisotropic nature of wood as well as differences between wood samples.  $R_f$  of native spruce wood varied between 1.0 and 1.5 and decreased with the oil content down to values only slightly above 1.0 for pure oil coatings, indicating a smooth surface. This is in agreement with observations from Figure 7, where it was stated that higher oil contents decreased surface irregularities as well as the observations from SEM (Figure 6). The obtained values seem reasonable when compared to literature values by Seo et al., who reported roughness factors of  $R_f = 1.63$  and 1.03 for a superhydrophobic surface and a moderately hydrophobic reference sample.<sup>13</sup>

The Wenzel equation eq 2 clarifies the importance of the roughness factor on the wettability of a surface. For the wetting regime in which a water drop is in full contact with the underlying hydrophobic surface, it states that the observed static water contact angle  $\theta$  increases with the roughness factor.<sup>41</sup>

$$\cos \theta = R_f \cos \theta_0 \quad (2)$$

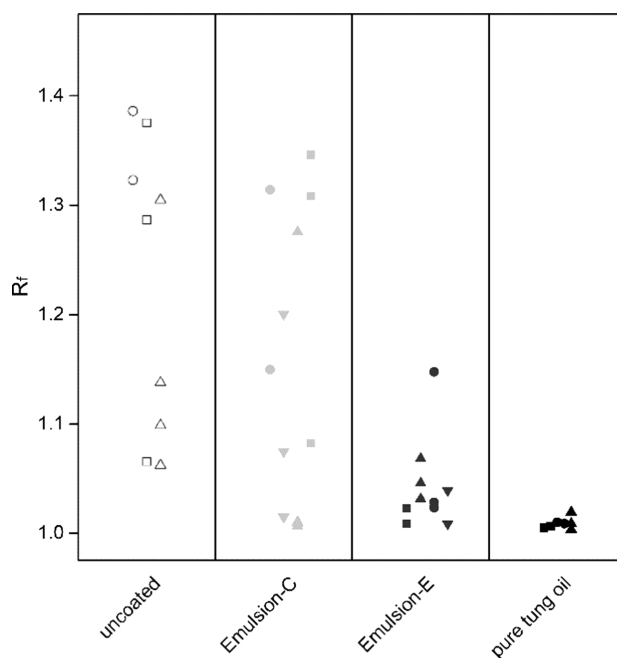


**Figure 8.** Roughness factor  $R_f$  for uncoated spruce wood and for spruce wood coated with tung oil emulsions and pure tung oil. Emulsion-E was prepared by dispersing 5 g of the binder mixture in deionized water. The oil content of Emulsion-C is about 25 times less than in Emulsion-E. Different wood samples within one group are distinguished by different symbols.

The higher roughness factor of coatings prepared from Emulsion-C could thus contribute to the higher initial WCA over coatings with a higher oil content (Figure 4). The Supporting Information gives details on limitations of comparability of samples used in the AFM study. For a more in-depth discussion on the relationship between surface roughness and hydrophobicity, please refer to the literature.<sup>42,43</sup>

**Results of Color Change and Gloss Measurements.** Measurements of color and gloss were carried out for samples coated with tung oil emulsion Emulsion-C, pure tung oil, and uncoated reference samples immersed only in deionized water. The exact oil content of Emulsion-C was 0.15 wt %. This concentration was deliberately chosen because contact angle measurements revealed good hydrophobic properties of coatings prepared from Emulsion-C (Figure 4). It was found that immersing samples into deionized water decreased their gloss values from 11 to around 6, which is likely a result of grain raising. The gloss of samples coated with Emulsion-C and spruce samples dipped into deionized water was similar with values of 6.1 and 5.8 gloss units at 60°, respectively. On the other hand, the gloss was strongly increased for samples coated with pure tung oil, indicated by values of ~22 gloss units.

Figure 9a shows results of color change measurements in the 3d CIELAB color space. The mean total color change  $\Delta E$  was 0.4 for reference samples, 0.8 for Emulsion-C, and 7.1 for pure tung oil coatings. While color differences of  $\Delta E < 1$  are not detectable for a human observer,  $\Delta E > 5$  is perceived as a different color.<sup>44</sup> It was thus concluded that coating spruce wood with low oil content Emulsion-C led to negligible differences in the color and gloss compared to uncoated control samples.

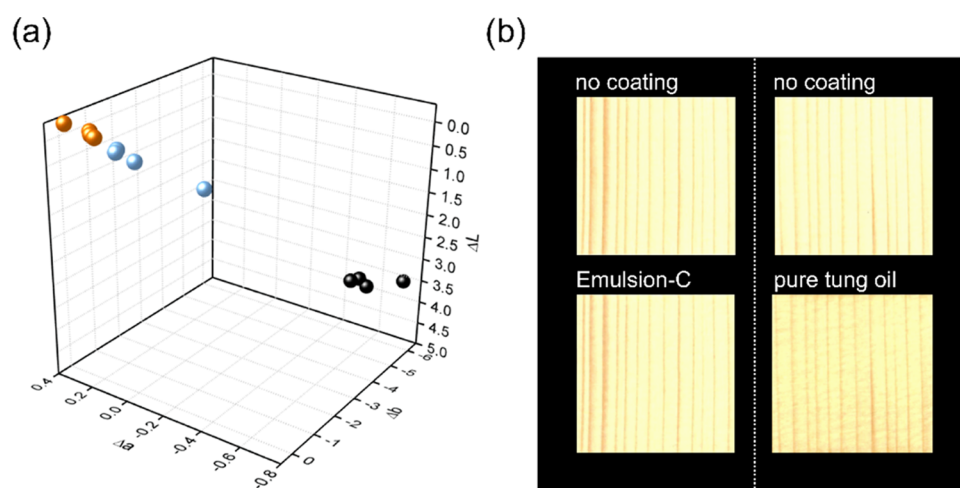


**Figure 9.** (a) Color change due to coating visualized in the 3d CIElab color space of control samples immersed into deionized water (orange) and samples coated with dilute Emulsion-C (blue) and pure tung oil (black). (b) Scans of spruce samples before coating (top), after coating with Emulsion-C (bottom left), and after coating with pure tung oil (bottom right).

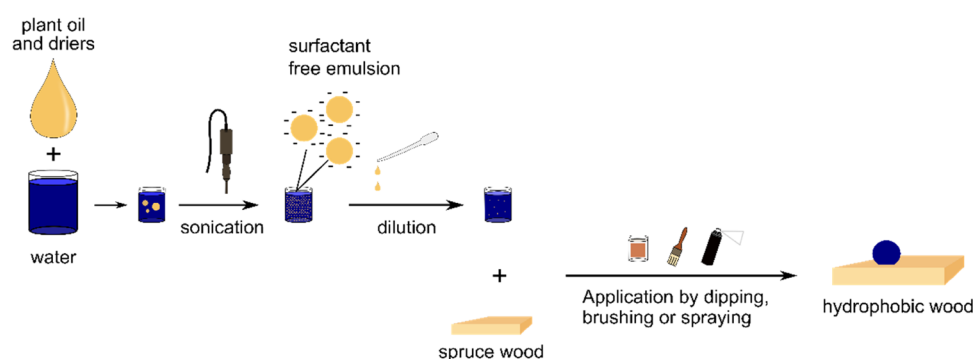


**Figure 10.** Graphical description of the emulsion preparation and the wood coating process.

Color changes due to coating with pure tung oil are well visible in scans of the surface before and after coating (Figure 9b). Just as with tung oil, also coatings based on other traditional finishes come with a change in optical properties. Transparent coatings based on alkyd or polyurethane easily reach gloss values above 35 GU and up to over 90 GU.<sup>45,46</sup> Compared to the emulsion-based coatings, herein, traditional coatings often use far higher surface coverages above  $100 \text{ g m}^{-2}$ ,<sup>46</sup> which is a likely reason for such changes. On the other hand, (super-)hydrophobic coatings based on the creation of nanostructures or microstructures may often lead to whitening of the surface and a reduction of gloss, which was also found true by two previous studies of our colleagues and group.<sup>8,21</sup>

## CONCLUSIONS

Self-stable surfactant-free emulsions from renewable, nontoxic plant oil and a derived alkyd resin were prepared by sonication and used to turn wood surfaces hydrophobic using a mass-efficient process. Tung emulsions with low oil contents of 0.04 and 0.16 wt %, corresponding to roughly 0.04 to  $0.15 \text{ g m}^{-2}$ , were highly effective in providing water repellency, yielding higher initial water contact angles than pure tung oil coatings. It was hypothesized that this was the result of preserved micro- and nanoroughness intrinsic to wood. Observations from scanning electron microscopy imaging and atomic force microscopy measurements support this hypothesis. In addition to endowing wood with good water repellency, dilute tung oil

emulsions had minimal impact on surface gloss and did not change the perceived color of coated wood, indicated by color differences of  $\Delta E < 1$ .

Thus, the use of such small amounts of oil preserves wood's esthetic properties, saves material, and provides hydrophobicity by conservation of wood's intrinsic complexity. Moreover, the use of nontoxic biodegradable materials facilitates recycling and after-life use of the coated wood. This study demonstrates an economic and highly efficient process, uniting several principles of green engineering.

## EXPERIMENTAL SECTION

**See Supporting Information for Experimental Details. Synthesis of the Alkyd Resin.** The procedure is based on the long oil alkyd synthesis described by Nalawade.<sup>47</sup> Briefly, 60 g of linseed oil, 13.47 g of glycerol, and 0.042 g of LiOH were heated under a nitrogen atmosphere. Following the addition of 21.6 g of phthalic anhydride, the reaction was heated until reaching an acid value of 11 mg of KOH/g resin, as determined by titration.

**Emulsion Preparation.** Tung oil, linseed oil, or alkyd resin were combined with the siccative and thoroughly mixed. Used concentrations were 0.25–0.5 wt % of 7% AOC E and Deca Zirconium containing siccative and  $\sim 1.5$  wt % of OXY-Coat 1410, which are based on Al, Zr, and Fr, respectively. Emulsification of 1 g of this mixture in 99 g of deionized water and 5 g in 95 g of deionized water gave emulsions with

different oil contents (Figure 10). Sonication was performed with a Q500 Sonicator (Qsonica) for a total duration of 10 min (5/15 s pulse) and 80% amplitude while being continuously stirred. The nonemulsified top layer of oil was rejected and the bottom part of the emulsion was transferred to a beaker with a pipette, which was repeated twice. Emulsions of lower concentrations were prepared by diluting the low concentration emulsion obtained by emulsification of 1 g of oil with deionized water, aiming for 5-fold, 20-fold, and 50-fold dilutions of the stock emulsion. In some experiments, the final oil content of the emulsions was determined gravimetrically by evaporation of the water phase at 70 °C. Because drying oil mass can slightly change due to curing, this is to be understood as an approximate mass.<sup>48</sup> An overview of the different emulsions with their corresponding oil content is shown in Table 1.

**Table 1. Terminology of Formulations Used for Coating Experiments with Tung Oil Together with their Oil Content and Estimated Surface Coverage Achieved**

formulation	preparation	oil content (wt %)	estimated coverage (g m <sup>-2</sup> )
uncoated	none	0	0
Emulsion-A	1 g oil/99 g water, diluted 50-fold	~0.01	0.01
Emulsion-B	1 g oil/99 g water, diluted 20-fold	~0.04	0.04
Emulsion-C	1 g oil/99 g water, diluted 5-fold	0.12–0.16	0.15
Emulsion-D	1 g oil/99 g water	0.7–0.8	1
Emulsion-E	5 g oil/95 g water	2.9–4.0	3–4
pure oil	none	100	10–30

**Wood Coating Procedure.** European spruce (*Picea abies*) was cut into specimens having dimensions of 40 × 40 mm<sup>2</sup> in longitudinal and radial directions and an approximate thickness of 5 mm. If not stated otherwise, the radial surface was successively sanded with sandpaper down to 600 grit. The samples were conditioned at 20 °C and 65% relative humidity prior to use.

In most experiments, tung oil emulsions were used because of the advantageous properties of this natural oil revealed in an earlier study.<sup>21</sup> Whenever emulsions of other oils were used, this was explicitly stated. In the general procedure, spruce samples were bath-coated by immersing them into the respective emulsion for 30 s and drying for 10 min at 60 °C. To coat wood with pure tung oil, oil was distributed to cover the entire wood surface. After 30 s, excess oil was wiped off. All coated samples were stored at 20 °C and 65% for a minimum of 7 days before further testing.

The amount of coating deposited on the surface was estimated in terms of g m<sup>-2</sup> from the approximate mass gain of specimens due to immersion for 30 s into deionized water, taking into account the oil content of the coating variant applied.

**Characterization of Coating Emulsions and Wood Samples. Characterization of the Emulsions.** Of each of the two oils and the alkyd resin, the emulsion of 1 g in 99 g water was diluted to a concentration of 1:99 with a 5 mM NaCl solution, and the  $\zeta$ -potential was tested using a Zetasizer Nano ZS (Malvern Panalytical).

**Surface Elemental Composition by X-ray Photoelectron Spectroscopy.** X-ray photoelectron spectroscopy (XPS) spectra were recorded to determine the elemental surface composition of wood and coated wood samples as well as the chemical states of carbon. Details are given in the Supporting Information. To achieve optimum comparability, analysis was performed on three locations of one wood specimen, these locations being either coated with Emulsion-C, pure tung oil, or left uncoated.

**Static Water Contact Angle of Coated Wood Samples.** The static water contact angle was measured 10 s after deposition of ~5  $\mu$ L water droplets using a Drop Shape Analyzer—DSA 30S (Krüss GmbH, Hamburg, Germany). Water contact angle stability was observed over the course of 120 s and 30 min, with data points being taken at intervals of 2 and 10 s, respectively (see the Supporting Information).

**Scanning Electron Microscopy Imaging.** Coated and uncoated spruce wood samples were sputter-coated with a 10 nm platinum layer using the instrument EM ACE200 (Leica). A tabletop electron microscope 3030 (Hitachi) was used for SEM imaging.

**Atomic Force Microscopy Measurements.** Atomic force microscopy (AFM) measurements of scan size 2 × 2  $\mu$ m<sup>2</sup> were performed at several locations on the surfaces of native wood and wood coated with Emulsion-C (low oil content), Emulsion-E (intermediate oil content), and pure tung oil (high oil content) using a Dimension Icon atomic force microscope. Details can be found in the Supporting Information.

**Measurements of Gloss and Color.** Gloss was measured on four locations per sample at an angle of 60° using a glossmeter (BYK-Gardner micro-TRI-gloss, BYK-Gardner GmbH). The CIELAB color of spruce wood samples before and after coating was measured on five locations using a spectrophotometer PCE-CSM 8 (PCE Instruments) with a standard observer angle of 10° and a D65 standard illuminant.

## ■ ASSOCIATED CONTENT

### Supporting Information

The Supporting Information is available free of charge at <https://pubs.acs.org/doi/10.1021/acsomega.1c02885>.

Details of the Experimental Section, graph of WCA stability over the course of 30 min, and information of AFM results section including height maps of all AFM scans used in this study (PDF)

## ■ AUTHOR INFORMATION

### Corresponding Author

Wolfgang Gindl-Altmutter – Wood K plus—Competence Centre for Wood Composites & Wood Chemistry, Kompetenzzentrum Holz GmbH, 4040 Linz, Austria; Department of Materials Sciences and Process Engineering, BOKU—University of Natural Resources and Life Sciences Vienna, 3430 Tulln, Austria; [orcid.org/0000-0002-8224-6762](https://orcid.org/0000-0002-8224-6762); Phone: +43 1 47654-89111; Email: [wolfgang.gindl@boku.ac.at](mailto:wolfgang.gindl@boku.ac.at)

### Authors

Jan Janesch – Wood K plus—Competence Centre for Wood Composites & Wood Chemistry, Kompetenzzentrum Holz GmbH, 4040 Linz, Austria; Department of Materials Sciences and Process Engineering, BOKU—University of

Natural Resources and Life Sciences Vienna, 3430 Tulln, Austria

**Claudia Gusenbauer** – Department of Materials Sciences and Process Engineering, BOKU—University of Natural Resources and Life Sciences Vienna, 3430 Tulln, Austria;

orcid.org/0000-0003-3520-3732

**Andreas Mautner** – Polymer and Engineering (PaCE) Group, Institute of Materials Chemistry and Research, Faculty of Chemistry, University of Vienna, 3090 Wien, Austria

**Christian Hansmann** – Wood K plus—Competence Centre for Wood Composites & Wood Chemistry, Kompetenzzentrum Holz GmbH, 4040 Linz, Austria

Complete contact information is available at:

<https://pubs.acs.org/10.1021/acsomega.1c02885>

### Author Contributions

This manuscript was prepared through the contributions of all authors. All authors have given approval to the final version of the manuscript. J.J. contributed to the planning, experimental work, and writing of the original manuscript; C.G. contributed to AFM investigation; A.M. contributed to XPS investigation and editing; W.G.-A. contributed to supervision and editing; and C.H. contributed to supervision.

### Notes

The authors declare no competing financial interest.

### ACKNOWLEDGMENTS

The federal state of Lower Austria is acknowledged for funding this research (Grant No. K3-F-670/003-2017). The authors thank Armin Winter, Stefan Veigel, and Gerhard Emsenhuber for their technical support. They further thank the Institute of Environmental Biotechnology for enabling the use of the scanning electron microscope, the sputter coater, and the Zetaser.

### REFERENCES

- (1) Rowell, R. M.; Banks, W. B. *Water Repellency and Dimensional Stability of Wood*, Gen. Tech. Rep. FPL-50, U.S. Department of Agriculture, Forest Service, Forest Products Laboratory, Madison, WI, 1985; p 24.
- (2) Brischke, C.; Alfredsen, G. Wood-water relationships and their role for wood susceptibility to fungal decay. *Appl. Microbiol. Biotechnol.* **2020**, *104*, 3781–3795.
- (3) Bulian, F.; Graystone, J. A. Raw Materials for Wood Coatings (1) - Film Formers (Binders, Resins and Polymers). In *Wood Coatings: Theory and Practice*; Elsevier, Amsterdam, 2009; pp 53–94.
- (4) Saji, V. S. Wax-based artificial superhydrophobic surfaces and coatings. *Colloids Surf., A* **2020**, *602*, No. 125132.
- (5) Chen, C.; Chen, J. Y.; Zhang, S. D.; Cao, J. Z.; Wang, W. Forming textured hydrophobic surface coatings via mixed wax emulsion impregnation and drying of poplar wood. *Wood Sci. Technol.* **2020**, *54*, 421–439.
- (6) Lozhechnikova, A.; Vahtikari, K.; Hughes, M.; Osterberg, M. Toward energy efficiency through an optimized use of wood: The development of natural hydrophobic coatings that retain moisture-buffering ability. *Energy Build.* **2015**, *105*, 37–42.
- (7) Lozhechnikova, A.; Bellanger, H.; Michen, B.; Burgert, I.; Osterberg, M. Surfactant-free carnauba wax dispersion and its use for layer-by-layer assembled protective surface coatings on wood. *Appl. Surf. Sci.* **2017**, *396*, 1273–1281.
- (8) Arminger, B.; Gindl-Altmutter, W.; Keckes, J.; Hansmann, C. Facile preparation of superhydrophobic wood surfaces via spraying of aqueous alkyl ketene dimer dispersions. *RSC Adv.* **2019**, *9*, 24357–24367.

(9) Hofland, A. Alkyd resins: From down and out to alive and kicking. *Prog. Org. Coat.* **2012**, *73*, 274–282.

(10) Hayden, D. R.; Papegaaij, A.; Reuvers, B.; Buijssen, P.; Koning, C. Sustainable, rigid imide building blocks as promising substitutes for phthalic anhydride in alkyd resins. *Polym. Int.* **2021**, *70*, 490–498.

(11) Arminger, B.; Jaxel, J.; Bacher, M.; Gindl-Altmutter, W.; Hansmann, C. On the drying behavior of natural oils used for solid wood finishing. *Prog. Org. Coat.* **2020**, *148*, No. 105831.

(12) Shah, S. M.; Zulfiqar, U.; Hussain, S. Z.; Ahmad, I.; Habib ur, R.; Hussain, I.; Subhani, T. A durable superhydrophobic coating for the protection of wood materials. *Mater. Lett.* **2017**, *203*, 17–20.

(13) Seo, K.; Kim, M.; Kim, D. H. Candle-based process for creating a stable superhydrophobic surface. *Carbon* **2014**, *68*, 583–596.

(14) Lu, X.; Hu, Y. C. Layer-by-layer Deposition of TiO<sub>2</sub> Nanoparticles in the Wood Surface and its Superhydrophobic Performance. *BioResources* **2016**, *11*, 4605–4620.

(15) Kong, L. Z.; Tu, K. K.; Guan, H.; Wang, X. Q. Growth of high-density ZnO nanorods on wood with enhanced photostability, flame retardancy and water repellency. *Appl. Surf. Sci.* **2017**, *407*, 479–484.

(16) Tan, S. X.; Xie, Q. D.; Lu, X. Y.; Zhao, N.; Zhang, X. L.; Xu, J. One step preparation of superhydrophobic polymeric surface with polystyrene under ambient atmosphere. *J. Colloid Interface Sci.* **2008**, *322*, 1–5.

(17) Choi, D.; Yoo, J.; Park, S. M.; Kim, D. S. Facile and cost-effective fabrication of patternable superhydrophobic surfaces via salt dissolution assisted etching. *Appl. Surf. Sci.* **2017**, *393*, 449–456.

(18) Poth, U. Drying Oils and Related Products. In *Ullmann's Encyclopedia of Industrial Chemistry*; Wiley, 2001; pp 621–634.

(19) Teng, T. J.; Arip, M. N. M.; Sudesh, K.; Nemoikina, A.; Jalaludin, Z.; Ng, E. P.; Lee, H. L. Conventional Technology and Nanotechnology in Wood Preservation: A Review. *BioResources* **2018**, *13*, 9220–9252.

(20) Xing, D.; Zhang, Y.; Hu, J. P.; Yao, L. H. Highly Hydrophobic and Self-Cleaning Heat-Treated Larix spp. Prepared by TiO<sub>2</sub> and ZnO Particles onto Wood Surface. *Coatings* **2020**, *10*, No. 986.

(21) Janesch, J.; Arminger, B.; Gindl-Altmutter, W.; Hansmann, C. Superhydrophobic coatings on wood made of plant oil and natural wax. *Prog. Org. Coat.* **2020**, *148*, No. 105891.

(22) Tu, K. K.; Kong, L. Z.; Wang, X. Q.; Liu, J. L. Semitransparent, durable superhydrophobic polydimethylsiloxane/SiO<sub>2</sub> nanocomposite coatings on varnished wood. *Holzforschung* **2016**, *70*, 1039–1045.

(23) Xu, Q. F.; Wang, J. N.; Sanderson, K. D. Organic-Inorganic Composite Nanocoatings with Superhydrophobicity, Good Transparency, and Thermal Stability. *ACS Nano* **2010**, *4*, 2201–2209.

(24) Wang, K. L.; Dong, Y. M.; Yan, Y. T.; Qi, C. S.; Zhang, S. F.; Li, J. Z. Preparation of mechanical abrasion and corrosion resistant bulk highly hydrophobic material based on 3-D wood template. *RSC Adv.* **2016**, *6*, 98248–98256.

(25) Ge, M. Z.; Cao, C. Y.; Liang, F. H.; Liu, R.; Zhang, Y.; Zhang, W.; Zhu, T. X.; Yi, B.; Tang, Y. X.; Lai, Y. K. A "PDMS-in-water" emulsion enables mechanochemically robust superhydrophobic surfaces with self-healing nature. *Nanoscale Horiz.* **2020**, *5*, 65–73.

(26) Council Directive 1999/13/EC on the limitation of emissions of volatile organic compounds due to the use of organic solvents in certain activities and installations. Official Journal of the European Union: 1999; pp 1–22.

(27) Kamogawa, K.; Akatsuka, H.; Matsumoto, M.; Yokoyama, S.; Sakai, T.; Sakai, H.; Abe, M. Surfactant-free O/W emulsion formation of oleic acid and its esters with ultrasonic dispersion. *Colloids Surf., A* **2001**, *180*, 41–53.

(28) Kaci, M.; Meziani, S.; Arab-Tehrany, E.; Gillet, G.; Desjardins-Lavis, I.; Desobry, S. Emulsification by high frequency ultrasound using piezoelectric transducer: Formation and stability of emulsifier free emulsion. *Ultrason. Sonochem.* **2014**, *21*, 1010–1017.

(29) Beattie, J. K.; Djerdjev, A. M. The pristine oil/water interface: Surfactant-free hydroxide-charged emulsions. *Angew. Chem., Int. Ed.* **2004**, *43*, 3568–3571.

- (30) Kanicky, J. R.; Shah, D. O. Effect of degree, type, and position of unsaturation on the pK(a) of long-chain fatty acids. *J. Colloid Interface Sci.* **2002**, *256*, 201–207.
- (31) Badolato, G. G.; Aguilar, F.; Schuchmann, H. P.; Sobisch, T.; Lerche, D. Evaluation of Long Term Stability of Model Emulsions by Multisample Analytical Centrifugation. In *Surface and Interfacial Forces – From Fundamentals to Applications*; Springer, 2008; Vol. 134, pp 66–73.
- (32) Popescu, C. M.; Tibirna, C. M.; Vasile, C. XPS characterization of naturally aged wood. *Appl. Surf. Sci.* **2009**, *256*, 1355–1360.
- (33) Nzokou, P.; Kamdem, D. P. X-ray photoelectron spectroscopy study of red oak- (*Quercus rubra*), black cherry- (*Prunus serotina*) and red pine- (*Pinus resinosa*) extracted wood surfaces. *Surf. Interface Anal.* **2005**, *37*, 689–694.
- (34) Bulian, F.; Graystone, J. A. Operational Aspects of Wood Coatings: Application and Surface Preparation. In *Wood Coatings: Theory and Practice*; Elsevier, Amsterdam, 2009; pp 259–288.
- (35) Gibbons, M. J.; Nikafshar, S.; Saravi, T.; Ohno, K.; Chandra, S.; Nejad, M. Analysis of a Wide Range of Commercial Exterior Wood Coatings. *Coatings* **2020**, *10*, No. 1013.
- (36) Papp, E. A.; Csilla, C. Contact angle as function of surface roughness of different wood species. *Surf. Interfaces* **2017**, *8*, 54–59.
- (37) Fahlén, J.; Salmen, L. Cross-sectional structure of the secondary wall of wood fibers as affected by processing. *J. Mater. Sci.* **2003**, *38*, 119–126.
- (38) Lai, L.; Irene, E. A. Area evaluation of microscopically rough surfaces. *J. Vac. Sci. Technol. B* **1999**, *17*, 33–39.
- (39) Ramón-Torregrosa, P. J.; Rodríguez-Valverde, M. A.; Amirfazli, A.; Cabrerizo-Vilchez, M. A. Factors affecting the measurement of roughness factor of surfaces and its implications for wetting studies. *Colloids Surf., A* **2008**, *323*, 83–93.
- (40) Hongru, A.; Xiangqin, L.; Shuyan, S.; Ying, Z.; Tianqing, L. Measurement of Wenzel roughness factor by laser scanning confocal microscopy. *RSC Adv.* **2017**, *7*, 7052–7059.
- (41) Wenzel, R. N. Resistance of solid surfaces to wetting by water. *Ind. Eng. Chem.* **1936**, *28*, 988–994.
- (42) Bhushan, B.; Nosonovsky, M. The rose petal effect and the modes of superhydrophobicity. *Philos. Trans. R. Soc., A* **2010**, *368*, 4713–4728.
- (43) Nosonovsky, M.; Bhushan, B. Superhydrophobic surfaces and emerging applications: Non-adhesion, energy, green engineering. *Curr. Opin. Colloid Interface Sci.* **2009**, *14*, 270–280.
- (44) Mokrzycki, W.; Tatol, M. Color difference Delta E - A survey. *Mach. Graphics Vision* **2011**, *20*, 383–411.
- (45) Raychura, A. J.; Jauhari, S.; Prajapati, V. S.; Dholakiya, B. Z. Synthesis and performance evaluation of vegetable oil based wood finish polyurethane coating. *Bioresour. Technol. Rep.* **2018**, *3*, 88–94.
- (46) Demirci, Z.; Sonmez, A.; Budakci, M. Effect of Thermal Ageing on the Gloss and the Adhesion Strength of the Wood Varnish Layers. *BioResources* **2013**, *8*, 1852–1867.
- (47) Nalawade, P. Alkyd-Based High-Solid and Hybrid Organic Coatings. (Electronic Thesis or Dissertation) <https://etd.ohiolink.edu/> (accessed 2021-05-10).
- (48) Lazzari, M.; Chiantore, O. Drying and oxidative degradation of linseed oil. *Polym. Degrad. Stability* **1999**, *65*, 303–313.